Kinetics of low-temperature catalytic combustion of ethylene at wet conditions for postharvest storage applications

Natalia Semagina,[1]* Rosanne Tam,[1] James Sawada[2]*

[1] Department of Chemical and Materials Engineering, University of Alberta, 9211-116 St. Edmonton Alberta T6G 1H9 Canada.; [2] Climacteric Controls Solutions, Inc. Edmonton, Alberta

Corresponding authors: jim.sawada@climacteric-controls.ca; semagina@ualberta.ca

Running title: Ethylene combustion

Keywords: VOC; catalytic combustion; palladium; ethylene combustion; postharvest storage; kinetic modeling

Abstract

The study addresses the reduction of ethylene levels in postharvest storage applications using a Pd-Zn-Sn/TiO_2 catalyst, which is capable of reacting trace concentrations of ethylene at temperatures as low as 278 K and at relative humidity as high as 90%. The rate law is derived from data collected using a constant volume batch reactor and a model for a storage room with associated packed bed reactor is developed. The amount of catalyst required to maintain an ethylene concentration of 0.1 ppmv in a room containing 20 tons of fruit having an ethylene metabolism of 0.1 ul/kg hr was calculated as a function of air temperature and water content. While the catalyst is capable of continuously removing ethylene from saturated, refrigerated air, the amount of catalyst required can be reduced significantly by incorporating conventional air conditioning solutions upstream of the catalyst bed. Such combined systems and their functions are discussed.

1. Introduction

The presence of ethylene in postharvest environments contributes to food waste. Because ethylene controls the senescence, or aging, of many plant species the presence of even trace concentrations of ethylene can significantly reduce the lifetime of postharvest fresh fruits and vegetables in storage and transport applications. Concentrations as low as 0.3 ppmv have been shown to reduce the postharvest lifetime of a range of perishables by up to 50%.[1]

While ethylene can be introduced into postharvest environments through the incomplete combustion of fossil fuels or by microbial action in soils the predominant sources are endogenous. Climacteric fruits such as bananas, apples, and avocados generate ever increasing quantities of ethylene as part their autocatalytic ripening cycle. For climacteric fruits, a small amount of ethylene will stimulate the fruit to increase its metabolism and produce a greater amount of ethylene. This increased concentration of ethylene will likewise provoke the fruit to metabolize even greater quantities of the gas and this process, left unchecked, will continue quasi-exponentially until the fruit is fully ripe.[2]

The effects of ethylene accumulation are felt by a range of postharvest operations. Fresh fruit and vegetable distributors can see ethylene associated with relatively low value commodities like bananas put pressure on higher value leafy greens and ornamental flowers. The vast quantities of tropical fruits shipped around the world by refrigerated ocean containers (reefers) risk arrival problems if the concentration of ethylene in the container rises to the point where the fruit arrives too ripe to be marketable. Deciduous fruit storage operations place hundreds of tons of deciduous fruit into hermetically sealed, controlled atmosphere rooms for up to 12

months. The conditions in the room are tailored to slow the metabolism of the fruit and reduce its sensitivity to ethylene but the sheer volume of fruit contained in the room ensures that ethylene concentrations will rise over time and risk overwhelming the mitigation measures. In all such postharvest storage and transportation applications the continuous removal of ethylene would help safeguard against metabolic disorders caused by rising ethylene concentrations.

Combustion catalysts are highly effective at removing trace organics from humid air. They use and create no toxic chemicals and have an effectively limitless capacity for ethylene. Closed-loop catalytic combustion systems specifically designed for ethylene removal in postharvest applications have been developed.[3] Such systems bring the ethylene-contaminated air into a device which heats the air to about 523 K, passes the gas through a catalyst bed which decomposes the ethylene to carbon dioxide and water, and returns the treated air through a heat exchange assembly to recover most of the heat. The heat exchange is necessary in postharvest applications to limit the temperature difference between the systems' exhaust air and the ambient temperature of the store. The primary drawback of these systems is the high power demand necessary to drive the heaters and associated equipment in the device. The high power demand of high temperature catalytic combustion systems generally limits them to stationary storage applications.

Reducing the operating temperature of an ethylene catalytic combustion system would directly reduce the power requirements for the system and would allow catalytic combustion systems to be considered for both larger and smaller postharvest transport and storage applications. A

number of examples of catalysts have been reported that have demonstrating the ability to react ethylene,[4–6] including at low temperatures. It is known that the presence of water vapour in the air stream creates competitive molecular species on the surface of the catalyst which reduces the main reaction rate.[7–10] To date, there have been no reports on the low temperature catalytic combustion of ethylene from an air stream containing a significant amount of water vapour.

Recently, one of us (J. Sawada) developed and patented[11] a novel, water vapour tolerant combustion catalyst that is capable of catalytically combusting ethylene at temperatures as low as 278 K and at humidity as high as 99+%. In this work, we investigate the ethylene combustion reaction kinetics over the Pd-Zn-Sn/TiO_2 catalyst at temperatures between 278 and 295K and up to 88% relative humidity. The obtained rate law was incorporated into a sealed fruit storage room design model with a packed bed reactor to establish the amount of catalyst required to continuously maintain a specified ethylene concentration. The catalyst quantity was calculated as a function of temperature and water concentration using a set of fixed conditions described herein.

2. Experimental methods

2.1. Catalyst preparation

A sodium titanate support was prepared through the hydrothermal treatment of crystalline TiO_2. A crystalline nano-scale TiO_2 powder (having a mean particle size of around 10 nm) was blended with water to make a slurry. This slurry was then added to a mixture of sodium silicate and sodium hydroxide. The mole ratio of reagents was selected such that the Ti/Si ratio was

approximately 10 and the Na/Ti ratio was approximately 1.5. Water was present as an excess reagent and the H_2O/Ti mole ratio was over 12. The mixture was homogenized and charged into an autoclave where it was stirred and heated at a temperature between 353 to 383 K for a period of about 24 hours. The resulting slurry containing the sodium titanate was partially neutralized using acid and then filtered and washed. The resulting filter cake was dried at 333 K and equilibrated in air before use. The mass of titanate used to prepare a catalyst composition was based on the as-weighed mass of the substrate dried and equilibrated under the specified conditions. No adjustments were made for water adsorbed on the surface of the support.

A catalyst composition containing 4 wt% Pd and 5 wt% Sn and 2 wt% Zn was prepared by adding 2.01 g of sodium titanate to 75 mL of water. The mixture was stirred to create a suspension. To this suspension was added a solution of 0.278 g $Pd(NO_3)_2$ dissolved in 30 mL of deionized water. The resulting mixture was stirred for roughly one hour before a solution containing 0.289 g of $Zn(NO_3)_2 \cdot 2H_2O$ dissolved in 30 mL of deionized water was added to the stirred mixture. The bimetallic mixture was then stirred continuously at ambient temperature for an addition hour. A solution of 0.210 g of $SnCl_2 \cdot 2H_2O$ was then added to the stirred suspension and the trimetallic mixture stirred for an additional hour. The cocoa-coloured suspension was filtered, washed with approximately 200 mL of deionized water, and left under ambient conditions until the filter cake was dry. Energy dispersive X-ray spectroscopic measurements (EDX) was performed on the dried catalyst which confirmed that the catalyst was composed of 4% Pd, 4.9% Sn, and 2.2% Zn with a residual 1.7 wt% quantity of residual Na. The BET specific surface area, determined by the N_2 adsorption, was found to be 205 m^2/g, with an average pore diameter of 4 nm.

2.2. Reactor system for kinetic studies

An isothermal constant-volume batch reactor (CVBR) was constructed to measure the rate of reaction of the catalyst under a range of conditions. **Error! Reference source not found.** shows the schematic of a test system. A diaphragm pump (KNF Model UNMP850KNDC) was used to circulate the gas through the system and the composition of the gas was measured at specified intervals using and SRI 8610 GC equipped with a flame ionization detector. The GC was configured with a stainless steel sample loop having a volume of roughly 1 mL and a 3.3 m Hayesep D column. Gases were eluted from the column isothermally at 358 K using a He flow rate of 25 ml/min through the column.

The test system was built into a chest freezer which was controlled (± 1 °) using an external digital temperature controller using feedback from a thermistor connected to the accumulation tank. An O_2 sensor (Mettler Toledo InPro 6800 Gas) was connected inline as was a temperature/RH logger (SensorPush) which was contained within an home-built, air-tight housing. The accumulation tank was a 1 US gallon stainless steel cylinder which was plumbed to the catalyst bed/bypass system with 0.00635 m (¼)" stainless steel line and compression fittings (Swagelok). All valves were 0.00635 m (¼") stainless steel manual ¼-turn shut off or 3-way ball valves (Swagelok). The fruit chamber was a 0.002 m^3 glass vessel fitted with an air-tight lid having with three ¼" bulkhead connectors; one for the air to leave, one to return, and one (fitted with a shut off valve) to inject a tracer gas to measure the base leak rate of the system.

The catalyst bed was constructed of a 0.0762 m (3”) section of 0.009525 m (3/8”) OD stainless steel tubing and was filled with roughly 0.5 g of binderless 20-40 mesh catalyst granules. The granules were packed between two plugs of glass wool and tapped to densify the bed. The resulting length of the catalyst bed was roughly 1 cm. The bypass and all other piping was constructed of 0.00635 m (¼)” stainless steel tubing.

The volume of the system was measured pycnometrically by disconnecting the fruit chamber at Valve 1 and connecting a known volume, charged to a known pressure, in its place. The known volume element was equipped with a pressure sensor. With Valve 1 off, Valve 2 positioned to flow to the tank, Valve 3 open, and Valve 4 directed to the catalyst bed, all piping and components in the batch reactor were in fluid contact. The volume of the system was measured through volume expansion. The pycnometer was charged to a known pressure (P1) with dry air and then Valve 1 was opened and the pressure decayed from P1 to P2. Because the whole system was isothermal when the measurements were taken, the volume of the test system can be calculated using a simplified PVT expression. It was determined that the volume of the accumulator and associated piping and fittings was 4.3 L.

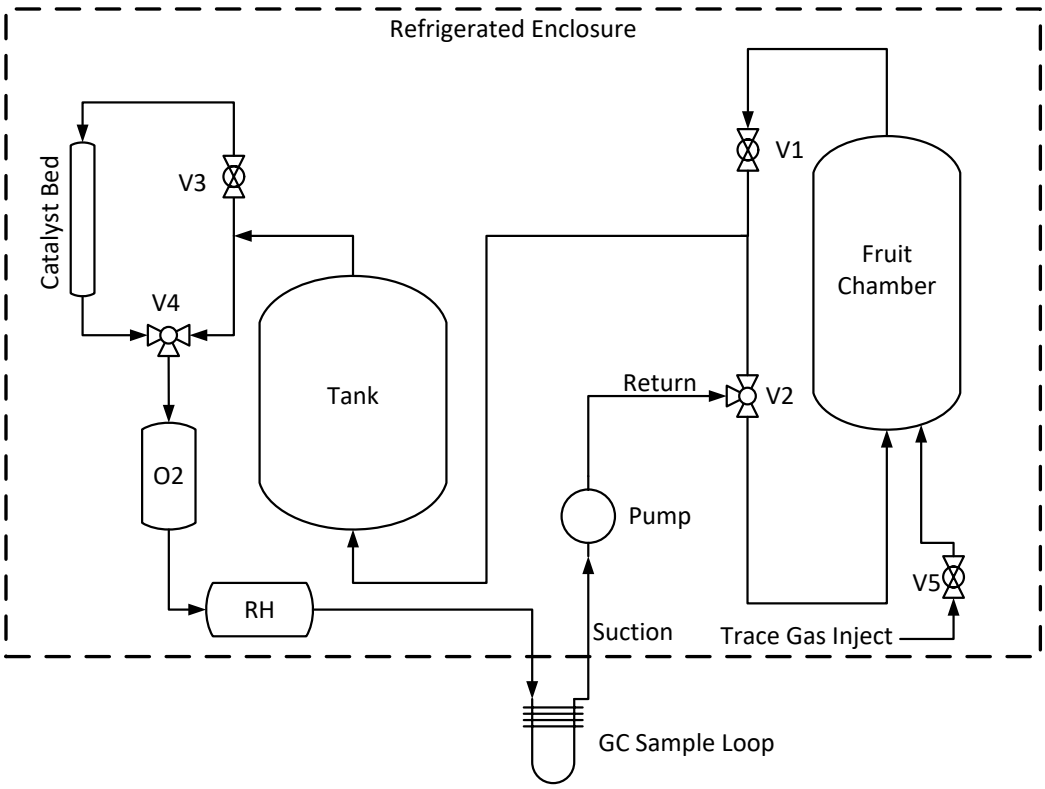

Figure 1. Schematic of the recirculating CVBR used for kinetic studies.

To accumulate ethylene (along with co-produced organic species), the fruit chamber was loaded with a number of avocado (cv. Hass). Once the fruit chamber was hermetically sealed, Valve 1 was opened, Valve 3 was closed and Valves 2 and 4 were positioned so that the air would circulate through the tank between the fruit chamber and the catalyst bypass line. Roughly 5 mL of 1% ethane (balance N_2) was injected via syringe to the fruit chamber through Valve 5 to provide a trace gas in the system. With the tracer gas injected, Valve 5 was closed and the recirculation pump was started. For experiments at 278 K and 291 K the freezer lid was closed and the enclosure cooled to the target temperature before starting the recirculation

pump. Ambient temperature was 295 K and for these experiments the lid to the freezer was left open so that the system could equilibrate to the room temperature.

The concentration of ethylene and ethane could be monitored over time by analyzing the composition of the gas continuously flowing through the GC sample loop. Endogenous ethylene was concentrated in the system by recirculating the air through the tank between the fruit chamber and the bypass line. During the accumulation step, the ethylene concentration in the system climbed over the course of about 18 hours to a point that where a significant amount of ethylene was no longer being produced. The cause of this metabolic slowdown was due to the progressive decrease in oxygen concentration in the system. After allowing the fruit to respire overnight, the O_2 concentration dropped to about 2% (absolute). It is expected that an associated increase in CO_2 was likewise produced during the respiration period but the GC did not have an onboard detector sensitive to CO_2 and so the precise concentration of this species remains unknown. An atmospheric composition of reduced O_2 and enriched CO_2 concentrations is similar to that used in controlled atmosphere (CA) storage rooms. The O_2 concentration in the system is still in vast excess compared to ethylene so the activity of the catalyst is not expected to be affected by the oxygen concentration in the system.

The ethane gas injected into the fruit vessel was used as a tracer to confirm that the change in concentration of ethylene in the system was due to the action of the catalyst and not due to a leak in the system. **Error! Reference source not found.** shows an example of the measured ethane concentration over time. The data in **Error! Reference source not found.** is typical and shows that for the duration of the experiment the concentration of ethane in the test system did not drift

significantly beyond the measurement uncertainty. The data in **Error! Reference source not found.** also serves to demonstrate the selectivity of the catalyst. By operating at low temperature, the activation energy for ethane is not reached and thus passes through the catalyst bed as a spectator species.

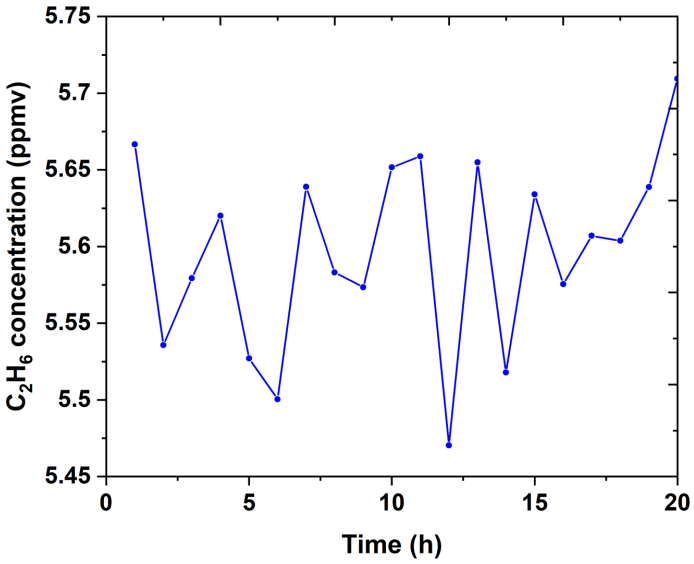

Figure 2. Measured ethane concentration as a function of time at 294 K.

The humidity in the system was at or very near saturation after the accumulation step was complete. For experiments which were carried out at lower humidity it was necessary to remove some of the water vapour in the system. To reduce the humidity, the pump was turned off, Valve 1 was closed and Valve 3 directed to recirculate between the tank and the bypass line. The fruit vessel was then replaced with a 25 g column of silica gel (Grace Davidson Grade 40) and the bed was connected to Valve 1 and Valve 3. With the silica gel bed in place, Valve 1

was opened, Valve 3 was directed to the silica gel bed and the recirculation pump was started. The gas was allowed to recirculate through the silica gel column for a period of time to remove a quantity of water vapour from the system. Once the RH sensor registered a change in RH, Valves 1 and 2 were actuated to direct the flow to the tank and away from the silica gel column. Once the RH sensor stabilized, if a lower RH was desired the flow was again directed to the silica gel bed and the flow switching process repeated until the desired RH was achieved. Once a stable humidity was reached, Valve 1 remained closed and Valve 2 remained directed toward the accumulation tank. The system was recirculated on bypass for one hour and gas samples were taken at 15 min intervals to ensure that the ethylene and ethane concentrations were stable.

For kinetic studies, Valve 3 was opened and Valve 4 was directed to the catalyst bed. In this configuration the accumulated ethylene is continuously drawn through the catalyst bed where some fraction of ethylene was catalytically combusted. The test gas was recirculated through the catalyst bed at ~ 33 $\mu m^3/s$ (STP) until a clear trend in the reduction of ethylene was evident. The majority of experiments were run overnight (~ 18 hours) though some where run for longer periods when the catalyst activity reached a degree where longer times were needed to get a clear trend. Gas samples were analyzed by the GC every 1 hour and the temperature and humidity were logged every minute.

The absence of mass and heat transfer limitations (MTL and HTL, respectively) was verified at the conditions where their affect would be the most dramatic, i.e., at the highest reaction temperature and low humidity (295 K, 24 RH%). The calculations followed the similar approach

as shown in ref. [12] Mears' criteria for external MTL amd HTL were found to be 10^{-3} and 10^{-8}, respectively, (below 0.15 to satisfy the requirement). Weisz-Prater criterion for the internal MTL was found to be 0.3 (below 0.6 to satisfy the requirement for a first-order reaction with effectiveness factor of 0.95). The internal temperature rise due to the exothermic combustion reaction was calculated to be 0.02 K and thus can be considered negligible. Thus, the reactions for kinetic studies were performed in intrinsic kinetic isothermal regime. The ideal plug flow profile can be assumed as well, as the ratio of the reactor to particle diameter exceeded 10, and the reactor Peclet number was above 10 for Bodenstein number of 0.7 at low Reynolds numbers.[13] The modeling was performed using Polymath.

3. Results and Discussion

3.1. Reaction kinetics

Figure 3 shows the plots for ethylene consumption as a function of time in the isothermal CVBR at different temperatures and relative humidity. Collectively, the data at 295 K show an increasing combustion rate as the water vapour in the system decreased. This result establishes that the reaction is inhibited by water; a phenomenon that has been noted for methane combustion over Pd catalysts. [14]

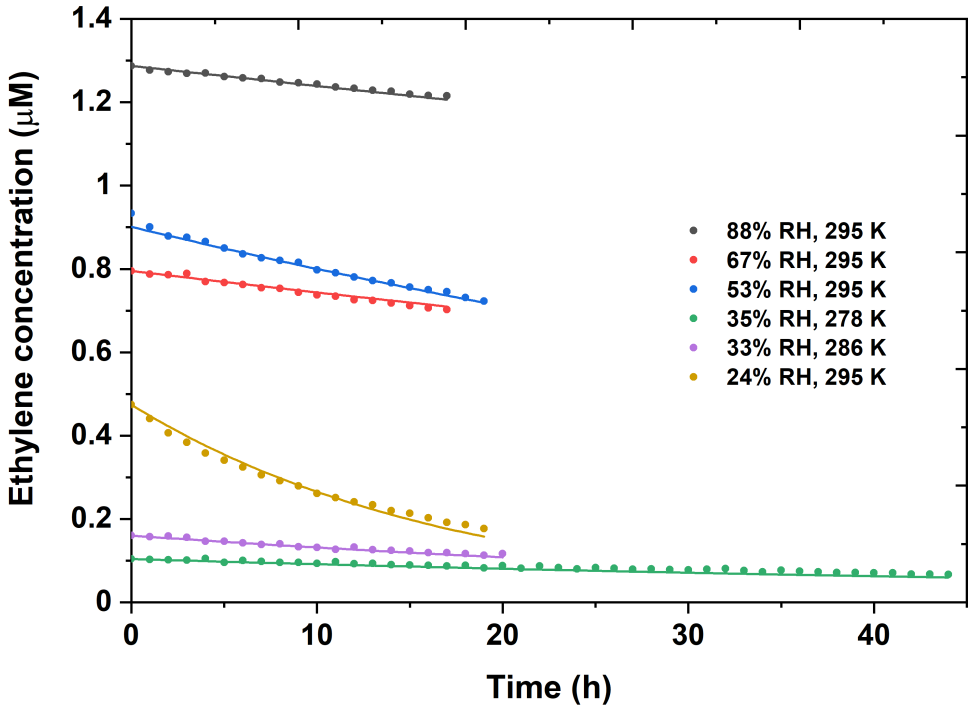

Figure 3. Experimental data (symbols) and simulated curves (lines) from the proposed rate law in Eq. (12).

To develop the rate law and determine the kinetic parameters for the reaction, the catalytic ethylene oxidation is suggested to occur similarly to Pd-catalyzed methane combustion via Langmuir-Hinshelwood mechanism. A single type of active site (S) is assumed. According to the mechanism, ethylene (E), oxygen and related oxidation products adsorb at the fractional coverage θ_i and quickly reach equilibrium at the adsorption constant K_i while the irreversible surface reaction remains the rate-determining step:

$$E + S \rightleftharpoons ES \qquad \theta_E = K_E C_E \theta_S \qquad (1)$$

$$O_2 + 2S \rightleftharpoons 2(OS) \qquad \theta_{Ox}^2 = K_{Ox} C_{Ox} \theta_S^2 \qquad (2)$$

$$ES + OS \rightarrow \cdots \rightarrow (CO_2)S + (H_2O)S \qquad r = k_{rxn} \theta_E \theta_{ox} \text{ (1st step is kinetically significant)} \qquad (3)$$

$$(CO_2)S \rightleftharpoons CO_2 + S \qquad \theta_{CO_2} = K_{CO_2} C_{CO_2} \theta_S \qquad (4)$$

$$(H_2O)S \rightleftharpoons H_2O + S \qquad \theta_{H_2O} = K_{H_2O} C_{H_2O} \theta_S \qquad (5)$$

The surface balance, assuming negligible coverage by intermediate oxidized species, becomes:

$$\theta_E + \theta_{ox} + \theta_{CO_2} + \theta_{H_2O} + \theta_S = 1 \qquad (6)$$

Assuming hydroxylated sites are the most abundant surface intermediates (as has been proposed for methane combustion[14]):

$$\theta_{H_2O} + \theta_S = 1 \qquad \theta_S = \frac{1}{1 + K_{H_2O} C_{H_2O}} \qquad (7)$$

the rate law in Eq. (3) becomes:

$$r = \frac{k_{rxn} K_E C_E \sqrt{K_{ox} C_{ox}}}{\left(1 + K_{H_2O} C_{H_2O}\right)^2} \qquad (8)$$

O_2 is present in significant excess and thus its concentration may be considered constant:

$$k = k_{rxn} K_E \sqrt{K_{ox} C_{ox}} \qquad (9)$$

The final rate law then becomes:

$$r = \frac{k C_E}{\left(1 + K_{H_2O} C_{H_2O}\right)^2} \qquad (10)$$

For a CVBR, the expression for the change in concentration of ethylene over time is:

$$-\frac{dC_E}{dt} = \frac{kC_E}{\left(1+K_{H_2O}C_{H_2O}\right)^2} \quad (11)$$

The ethylene combustion rate constant *k* dependence on temperature k follows the Arrhenius law while the water adsorption equilibrium constant K_{H2O} follows van't Hoff's law:

$$-\frac{dC_E}{dt} = \frac{k_o \exp\left(-\frac{E_a}{RT}\right)C_E}{\left(1+K_o \exp\left(-\frac{\Delta H}{RT}\right)C_{H_2O}\right)^2} \quad (12)$$

Fitting results of the experimental data to the rate law from Eq. (12) are shown in Fig. 3 (as lines) and Table 1.

Table 1. Modeling results of the experimental data in a CVBR as per **Error! Reference source not found.** and Eq. (12). The CVBR volume is 4.295 L, catalyst loading is 0.4771 g_{cat} (4 wt.% Pd). R^2 = 0.908.

Parameter in Eq. (12)	Value	95% confidence
k_o, h^{-1}	$9.60 \cdot 10^{12}$	$0.34 \cdot 10^{12}$
E_a, J/mol	42200	87
K_o, L/mol	2.66	0.05
ΔH, J/mol	-36970	43

The units of rate constant k in Eq. (11) and pre-exponential factor k_o in Eq. (12) are based on the CVBR volume. The specific reaction rate per catalyst mass [$mol_E/(kg_{cat} \cdot h)$] is

$$-r'_E = \frac{k'C_E}{\left(1+K_{H_2O}C_{H_2O}\right)^2} \quad (13)$$

with the rate constant $k'=k\cdot V_{gas\ in\ CVBR}/W_{cat} = k\cdot 4.295/0.4771 = 9.0023\cdot k$, [$m^3_{gas}/(kg_{cat}\cdot h)$].

Thus, the rate law describing the ethylene combustion on the catalyst with 4 wt%. Pd follows Eq. (14):

$$-r'_E = \frac{k'_o \exp\left(-\frac{E_a}{RT}\right) C_E}{\left(1+K_o \exp\left(-\frac{\Delta H}{RT}\right) C_{H_2O}\right)^2} \quad (14)$$

where $-r'_E$ is in units of $mol_E/(kg_{cat}\cdot s)$; $k'_o = 2.399\cdot 10^{10}$ $m^3_{gas}/(kg_{cat}\cdot s)$, $K_o = 2.66\cdot 10^{-3}$ m^3_{gas}/mol_{H2O}; E_a = 42200 J/mol; ΔH = -36970 J/mol; R = 8.314 J/(mol·K), T is in K; C_E and C_{H2O} in mol/m^3_{gas} (at reaction conditions, both are temperature-dependent).

3.2. Design of a sealed storage container

To calculate the quantity of catalyst needed to maintain a fixed ethylene concentration in a sealed postharvest storage container, the following constraints were placed on the model: the composition, volume, temperature, and humidity of the air in the fruit store was constant; the ethylene respiration rate of the fruit was constant; the gases mixed and behaved ideally; the catalytic reactor operated as an ideal packed-bed reactor (PBR) and had no heat or mass transfer limitations; the catalytic reactor achieved an ideal plug-flow profile absent of pressure drop and catalyst deactivation. To achieve this final requirement the catalyst would need to be suitably pelletized or formed into a monolithic structure like a honeycomb. Since the catalyst is prepared initially as a powder both of these assumptions are reasonable constraints.

Error! Reference source not found. summarizes the storage room design parameters with the used assumptions and notations.

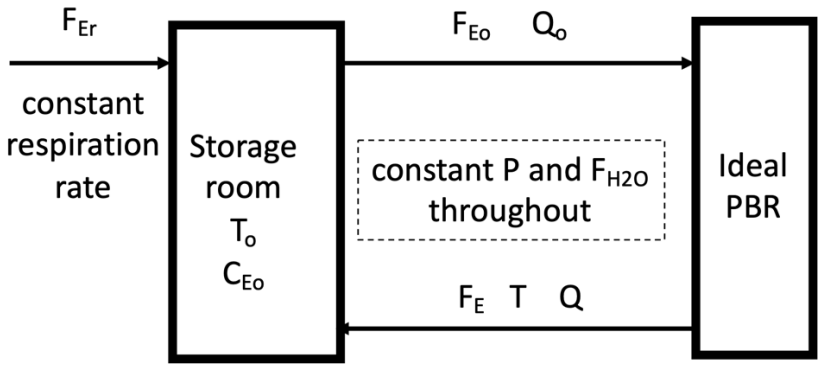

Figure 4. Storage room design parameters.

The mole balance for the ideal packed bed reactor (PBR) is:

$$\frac{dF_E}{dW} = r'_E \tag{15}$$

where [F_E] is the molar flow of ethylene expressed as [mol/s] and [W] is the catalyst charge expressed as [kg_{cat}].

Using weight-time τ' [kg_{cat} /m^3_{gas}] (volumetric flow rate Q_o is at the reactor entrance conditions):

$$\tau' = W/Q_o \tag{16}$$

the mole balance (15) can thus be rewritten as

$$\frac{dF_E}{d\tau'} = Q_o r'_E \tag{17}$$

The rate law and rate constants for the catalyst are given by Eq. (14).

The total molar flow rate of the gas mixture can be considered to be constant because ethylene is present only in trace amounts and the water vapour is not removed by the catalyst. The general equation for the water or ethylene concentrations under these conditions is expressed in Eq. (18) which accounts for the potential volumetric flow rate Q variation due to temperature or pressure variations along the PBR, where the subscript “o” refers to the reactor entrance conditions:

$$C_j = \frac{F_j}{Q} = \frac{F_j}{Q_o}\frac{P}{P_o}\frac{T_o}{T} \tag{18}$$

Assuming the reactor is well-insulated, the energy balance for an adiabatic PBR is expressed as:

$$\frac{dT}{dW} = \frac{r'_E \Delta H_{rxn}}{\sum F_j C_{p_j}} \tag{19}$$

where the denominator includes the temperature-dependent heat-capacities of all gas components C_{pj} (including inerts) and the heat of the ethylene combustion reaction at the reaction temperature and pressure. Since the heat of combustion for ethylene does not vary significantly within the temperature range studied the standard heat of the reaction at 298.15 K can be used. Because ethylene is a trace component in the stream, its contribution to the calculated heat capacity can be disregarded. The flow properties of the reactant stream can therefore be reasonably approximated as humid air. The specific constant pressure heat capacity for humid air of as 1.1 kJ/(kg·K) can be used as the average constant between 273 and 323 K

$$\frac{dT}{dW} = \frac{r'_E \Delta H^o_{rxn,298.15}}{\dot{m}\overline{C_{p,air}}} \quad (20)$$

The storage room mole balance for ethylene (assuming no ethylene accumulation) as per Fig. 4, is:

$F_{Er} + F_E - F_{Eo} = 0$, or $F_{Er} = F_{Eo} - F_E$ (21)

Equations (17), (18), (14), (20) and (21) can be solved simultaneously in an ODE solver with the output of F_{Er} vs. τ' to establish the catalyst weight-time needed to counterbalance the fruit respiration rate.

Under certain conditions, such as used for the kinetic studies, the temperature rise as per the Eq. (20) is negligible, which is due to the large dilution of ethylene with air. When the temperature rise in the adiabatic bed as per Eq. (20) is negligible, as in the case of the kinetic studies in Section 3.1, then isothermal reactor operation can be assumed. Thus, at a constant volumetric flow rate (in addition to the assumptions stated at the start of this section) the rate law from Eq. (14) can be simplified to:

$$-r'_E = A \cdot C_E \quad (22)$$

$$A = \frac{k'_o \exp\left(-\frac{E_a}{RT}\right)}{\left(1+K_o \exp\left(-\frac{\Delta H}{RT}\right) C_{H_2O}\right)^2} \quad (23)$$

where all the parameters are defined as per the variables provided with equation (14).

The PBR design equation becomes equation (24)

$$\frac{dF_E}{d\tau'} = Q_o r'_E \quad \text{or}$$

$$-\frac{dC_E}{d\tau'} = AC_E$$

and

$$C_E = C_{E_o} e^{-A\tau'} \quad (24)$$

The storage room balance (21) is simplified as

$$F_{E_r} = Q_o C_{E_o}(1 - e^{-A\tau'}). \quad (25)$$

F_{Er} vs. τ' can be thus evaluated to establish the weight-time needed to counterbalance the respiration rate.

To find the catalyst mass needed to combat a selected ethylene respiration rate and to maintain a desired ethylene concentration in the store Eq. (26) can be modified to:

$$W = \frac{Q_o}{-A} ln\left(1 - \frac{F_{E_r}}{Q_o C_{E_o}}\right) \quad (26)$$

3.3. Example of catalyst loading requirements in a sealed storage container

A postharvest transport scenario was selected to analyze the catalyst requirements for ethylene removal under a range of environmental conditions. The scenario selected used 20 metric tons of fruit enclosed in a container with a free volume of 40 m^3. In the scenario the fruit generated ethylene at a constant rate of 0.1 μL/(kg·h)[15] and the ethylene concentration to be maintained in the container was 0.1 ppmv. This scenario approximates a forty-foot refrigerated ocean container (commonly called a reefer) filled completely with boxes of fruit.

The flow rate to the reactor was fixed at 3 m^3/s. The temperature and humidity of the air entering the catalyst bed was varied between 278 and 318 K and the water concentration was varied between 0.0121 and 0.64 mol/m^3. The amount of catalyst required to meet the scenario described above was calculated for a range of points in the matrix. The results from these calculations are shown in **Error! Reference source not found.**.

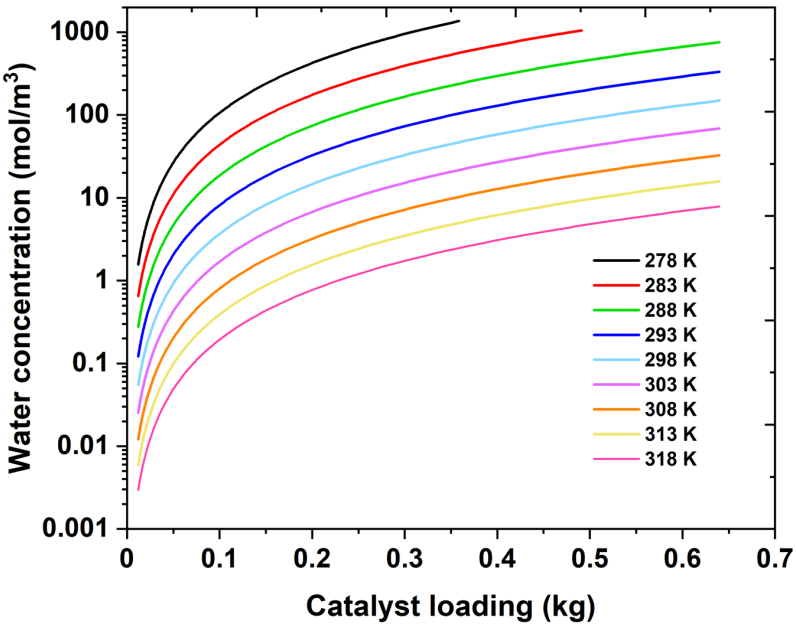

Figure 5. Dependence of the required catalyst loading on temperature at relative humidity to maintain 0.1 ppmv concentration in the storage room.

Figure 5 reveals the rate law described in Equation 23 and demonstrates that the combination of low temperature and high water concentration exponentially increases the demands on the catalyst. While the catalyst remains capable of continuously removing ethylene at 278 K and

near saturated humidity, the rate of reaction is too low to reasonably keep pace with 20 tons of fruit continually producing ethylene in a small, sealed enclosure.

As the water content in the air is reduced, the catalyst requirement falls dramatically. Starting at 278 K and a water content near saturation; if the water content is reduced by 95% the required amount of catalyst falls by orders of magnitude. Dehydration of the ethylene-contaminated air offers a simple mechanism by which to improve the efficiency of the combustion catalyst. A similar approach to dehydrate the stream before entering the combustion zone was demonstrated for methane combustion.[16]

Figure 5 also demonstrates the significant effect the temperature plays on the amount of catalyst required to maintain a fixed ethylene concentration. For example, at a constant water concentrationit can be seen that warming near-saturated air from 278 to 318 K reduces the catalyst requirement by 99.8%; a 550X reduction. If the air is also dried before warming the combination of effects would further minimize the catalyst requirement by driving the operating conditions toward conditions that favour the lowest catalyst requirements. The additional process complexity required to achieve simultaneous drying and warming would allow smaller catalyst beds to deal with larger quantities of perishables, higher ethylene metabolism rates, or to maintain lower target ethylene concentrations in the fruit store.

4. Conclusions

A kinetic study of ethylene combustion over Pd-Zn-Sn/TiO_2 catalyst was performed at temperatures between 278 and 295K and up to 88% relative humidity. The rate law was fit to the experimental data with the first order to ethylene and negative order to water. The

observed activation energy and heat of water adsorption were found as 42 and -37 kJ/mol, respectively. The obtained rate law was incorporated into a sealed fruit storage room design model with a packed bed reactor. The catalyst quantity was calculated as a function of temperature and water concentration to continuously maintain a specified ethylene concentration. The operation of an ethylene removal system at ambient temperature could be realized simply by pre-drying the inlet air stream. Greater reductions in catalyst loadings are possible by warming the gas and the greatest reductions in the size of the catalyst bed can be realized by simultaneously drying and warming the gas before introducing it to the catalyst bed.

5. Acknowledgements

Authors thank Roshni Sajiv Kumar for BET analysis of the catalyst sample.

References

1. Wills RBH, Warton MA, Ku VVV. Ethylene levels associated with fruit and vegetables during marketing. *Australian Journal of Experimental Agriculture*. 2000;40(3):465-470. doi:10.1071/ea99125

2. Wills RBH, Warton MA, Mussa DMDN, Chew LP. Ripening of climacteric fruits initiated at low ethylene levels. *Australian Journal of Experimental Agriculture*. 2001;41(1):89-92. doi:10.1071/EA00206

3. Wojciechowski J, Haber J, Gozdziewicz Z, Lange E. US Patent 4,506,599 (1985). Device for removal of ethylene from fruit storage chambers. Published online 1985.

4. Wang X, Lian M, Yang X, et al. Enhanced activity for catalytic combustion of ethylene by the Pt nanoparticles confined in TiO2 nanotube with surface oxygen vacancy. *Ceramics International*. Published online October 2021. doi:10.1016/j.ceramint.2021.10.180

5. Li W, Zhang Z, Wang J, Qiao W, Long D, Ling L. Low temperature catalytic combustion of ethylene over cobalt oxide supported mesoporous carbon spheres. *Chemical Engineering Journal*. 2016;293:243-251. doi:10.1016/j.cej.2016.02.089

6. Zhang Q, Zhu C, Gao J, et al. Microfibrous structured Au/Co3O4/Al-fiber catalyst for the combustion of ethylene traces. *Catalysis Communications*. 2020;146. doi:10.1016/j.catcom.2020.106133

7. Barrett W, Shen J, Hu Y, Hayes RE, Scott RWJ, Semagina N. Understanding the Role of SnO2 Support in Water-Tolerant Methane Combustion: In situ Observation of Pd(OH)2 and Comparison with Pd/Al2O3. *ChemCatChem*. 2020;12:944-952. doi:10.1002/cctc.201901744

8. Losch P, Huang W, Vozniuk O, Goodman ED, Schmidt W, Cargnello M. Modular Pd/Zeolite composites demonstrating the key role of support hydrophobic/hydrophilic character in methane catalytic combustion. *ACS Catalysis*. Published online 2019:4742-4753. doi:10.1021/acscatal.9b00596

9. Gholami R, Alyani M, Smith K. *Deactivation of Pd Catalysts by Water during Low Temperature Methane Oxidation Relevant to Natural Gas Vehicle Converters*. Vol 5.; 2015. doi:10.3390/catal5020561

10. Sajiv Kumar R, Hayes RE, Semagina N. Effect of support on Pd-catalyzed methane-lean combustion in the presence of water: Review. *Catalysis Today*. 2021;382:82-95. doi:10.1016/j.cattod.2021.07.024

11. Sawada J. Patent WO 2018/049512. Catalytic combustion in low temperature, humid conditions. Published online 2018.

12. Nassiri H, Lee KE, Hu Y, Hayes RE, Scott RWJ, Semagina N. Water shifts PdO-catalyzed lean methane combustion to Pt-catalyzed rich combustion in Pd–Pt catalysts: In situ X-ray absorption spectroscopy. *Journal of Catalysis*. 2017;352:649-656. doi:10.1016/j.jcat.2017.06.008

13. Gierman H. Design of laboratory hydrotreating reactors. Scaling Down of Trickle-flow Reactors. *Applied Catalysis*. 1988;43(2):277-286. doi:10.1016/S0166-9834(00)82732-3

14. Fujimoto KI, Ribeiro FH, Avalos-Borja M, Iglesia E. Structure and reactivity of PdOx/ZrO2 catalysts for methane oxidation at low temperatures. *Journal of Catalysis*. 1998;179(2):431-442. doi:10.1006/jcat.1998.2178

15. Kader AA. Fruit produce facts: Banana. 1996. https://postharvest.ucdavis.edu/Commodity_Resources/Fact_Sheets/Datastores/Fruit_English/?uid=9&ds=798. (Last accessed: November 28, 2021).

16. Huang W, Zhang X, Yang AC, Goodman ED, Kao KC, Cargnello M. Enhanced Catalytic Activity for Methane Combustion through in Situ Water Sorption. *ACS Catalysis*. 2020;10(15):8157-8167. doi:10.1021/acscatal.0c02087